Numerical simulation of a 4 K hybrid refrigerator combining GM gas expansion effect with magnetic refrigeration effect

Xiaohui Guo[a,b], Ke Li[a], Wei Dai[a,b*], Xinqiang Gao[a], Jun Shen[a,b], Wenchi Gong[a,b]

[a] Key Laboratory of Cryogenics, Technical Institute of Physics and Chemistry, Chinese Academy of Sciences, Beijing 100190, China

[b] University of Chinese Academy of Sciences, Beijing 100049, China

Abstract: A hybrid refrigerator (also named GM/Magnetic refrigerator) combining GM gas expansion effect with magnetic refrigeration effect has been proposed and experimentally proved to reach a higher cooling power than pure GM recently. Considering the complexity of thermodynamics and fluid dynamics of the hybrid refrigeration, optimizations based on numerical simulation are necessary to provide a useful guidance for the practical design. In this paper, a 2D axis-symmetric and transient numerical model of the hybrid refrigerator is established using COMSOL Multiphysics. With this model, the effect of the timing between gas expansion and magnetic refrigeration is studied and optimized. The corresponding cooling capacity and efficiency are obtained and compared with the results from pure gas expansion. The results showed that the optimal phase angle (the phase difference between the maximum value of varying magnetic field and the minimum value of varying expansion space volume) is 90°, which was very close to previous experimental results. The cooling power at 4 K increased from 0.13 W with pure gas expansion to 0.27 W with the hybrid scheme, and the efficiency improved by 2.13 times. The successful implementation of the numerical calculation with COMSOL will greatly help to optimize the performance of hybrid refrigerator. Meanwhile, a modification on thermal conductivity of porous media in COMSOL is proposed, which is important for a more accurate estimation of the cooling power.

Key words: GM/Magnetic refrigerator; numerical simulation; phase angle; performance evaluation

1. Introduction

The Gifford-McMahon (GM) [1] refrigerator based on gas expansion effect can provide a cooling temperature below 4.2 K using magnetic materials such as Er_3Ni and ErNi as regenerator materials [2]. They are widely used to cool superconducting magnets for applications such as magnetic resonance imaging and to provide low temperature environment for condensed matter physics research, etc. [3, 4]. A basic GM refrigeration cycle consists of four processes: compression, hot-to-cold blow, expansion and cold-to-hot blow. Due to the limited specific heat capacity of regenerator materials as well as non-ideal properties of helium at liquid helium temperature, the efficiency of GM refrigerator can only reach about 1% of the ideal thermodynamic efficiency [5].

Besides GM gas expansion, magnetic refrigeration [6] based on magnetocaloric effect (MCE) is another cooling method, which can reach sub-Kelvin temperature without helium [7]. Magnetocaloric material (MCM) is used as refrigerant and manifests change in temperature upon a changing magnetic field. When the operating temperature is below 1 K, the temperature span is narrow with a small cooling power requirement and magnetic Carnot cycle is used. As the operating temperature is around the ambient temperature, Brayton cycle based on active magnetic regenerator (AMR) is often used to obtain a larger temperature span with a much bigger cooling power. It also consists of four processes: magnetization, cold-to-hot blow, demagnetization and hot-to-cold blow [8].

Considering the intrinsic high efficiency of magnetic refrigeration and the similarity of thermodynamic cycles of the two refrigeration methods, a hybrid refrigerator [9] combining gas expansion and magnetic refrigeration was proposed, in which magnetic materials that have both appreciable specific heat capacity and magnetocaloric effect below 10 K are used as the lowest stage regenerator materials. A higher thermodynamic efficiency may be achieved through this configuration.

Based on the GM/Magnetic cycle, a hybrid refrigeration experimental device was built in 1995, and a no-load temperature of 4.5 K was obtained [10, 11]. This device is pre-cooled by liquid helium and does not include a complete GM refrigerator. In 1996, Yayama et al. developed a numerical model of GM refrigeration with ErNi as the regenerator material, and predicted a higher cooling power by applying a constant magnetic field [12]. The magnetocaloric effect is not considered in the model until 2000, they applied a time-varying magnetic field to the GM model to simulate the hybrid refrigeration, and predicted a larger cooling power than GM refrigeration [13]. In 2019, Shen et al. set up a hybrid refrigeration experimental device, with the lowest stage regenerator filled with ErNi and TmCuAl. The minimum no-load temperature was 3.5 K, which was lower than the 4.2 K obtained by GM refrigeration on the same setup [14]. Considering the complexity of thermodynamic cycle and fluid dynamics of the hybrid refrigeration system, it is difficult to analyze the physical mechanism only by observing the experimental results. To improve the efficiency of the hybrid refrigerator, optimization based on numeric simulation is necessary.

In this paper, a 2D axis-symmetric and transient numerical model of the hybrid refrigerator is established using COMSOL Multiphysics. A modified thermal conductivity of porous media is proposed to obtain a more accurate cooling power. With this model, the effect of the timing between gas expansion and magnetic refrigeration is studied and optimized. The corresponding cooling capacity and efficiency are obtained and compared with the results from pure gas expansion.

2. Simulation model

This section mainly describes the geometric model simplified from experimental device as well as the mathematical model.

2.1 Model description

Fig. 1 shows a 2D axis-symmetric geometric model of the hybrid refrigeration including a second stage regenerator and an expansion chamber. According to the experimental device we have built before, the main geometric and operating parameters of the model are shown in Table 1. The regenerator is filled with Pb and ErNi from high temperature side to low temperature side. A periodic sinusoidal magnetic field is applied to the regenerator section that contains ErNi.

The thermodynamic cycle of hybrid refrigeration consists of four processes. First is the expansion process. The bottom of the expansion chamber is fixed at the lowest point. The exhaust valve opens and the helium flows out. The temperature and pressure in the expansion chamber decreases. Second is the cold-to-hot blow/magnetization process. The bottom of expansion chamber moves upward, the helium continues to flow out and absorbs heat from regenerator materials. Meanwhile, the magnetic field increases, the magnetic entropy of ErNi decreases and the temperature increases, which enhances the ability to release heat to the helium. Third is the compression process. The bottom of the expansion chamber is fixed at the top point. The intake valve opens and the helium flows into the regenerator from high temperature side, the pressure and the temperature increase. Fourth is the hot-to-cold blow/demagnetization process. The bottom of expansion chamber moves downward. The helium continues to flow into the regenerator and releases heat to the regenerator materials. Meanwhile, the magnetic field decreases, the magnetic entropy of ErNi increases and the temperature decreases, which enhances the ability to absorb heat from the helium.

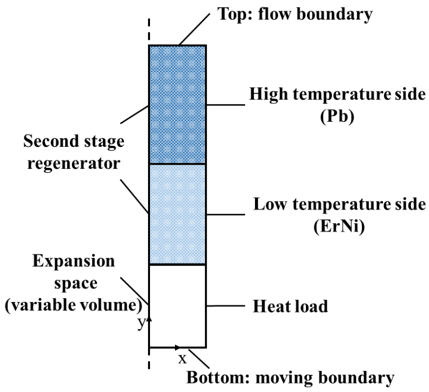

Fig. 1 Geometric model of the hybrid refrigeration

Table 1 Geometric and operating parameters of simulation model

Regenerator		High temperature side	Low temperature side
	Material	Pb	ErNi
	Mass	325 g	235 g
	Porosity	0.38	0.38
	Particle diameter	0.4 mm	0.4 mm
	Regenerator diameter	30 mm	30 mm
Expansion space			
	Diameter	30 mm	
	Stroke	35 mm	
	Bottom displacement curve ($y_0(t)$)	A sine curve (dotted line in Fig. 2)	
Operating parameters			
	Frequency	1 Hz	
	Inlet temperature (T_0)	45 K	
	Inlet pressure ($p_0(t)$)	0.6-2.4 MPa (solid line in Fig. 2)	
	Magnetic field ($\mu_0 H$)	0-1.1 T (dotted line in Fig. 3)	

2.2 Governing equations

The governing equations of the above model are as follows.

Continuity equation of helium

$$\frac{\partial \rho_{\mathrm{f}}(T_{\mathrm{f}}, p)}{\partial t} + \nabla \cdot \left(\rho_{\mathrm{f}}(T_{\mathrm{f}}, p)\mathbf{u}\right) = 0 \tag{1}$$

Momentum equation of helium

$$\frac{\partial\left(\rho_{\mathrm{f}}(T_{\mathrm{f}}, p)\mathbf{u}\right)}{\partial t} + \left(\rho_{\mathrm{f}}(T_{\mathrm{f}}, p)\mathbf{u}\cdot\nabla\right)\mathbf{u} + \nabla p - \nabla^2\left(\mu_{\mathrm{f}}(T_{\mathrm{f}}, p)\mathbf{u}\right) = 0 \tag{2}$$

The low temperature regenerator adopts the local thermal non-equilibrium model, and the energy equations of helium and regenerator materials in the regenerator are as follows.

$$\varepsilon\frac{\partial\left(\rho_{\mathrm{f}}(T_{\mathrm{f}}, p)c_{p,\mathrm{f}}(T_{\mathrm{f}}, p)T_{\mathrm{f}}\right)}{\partial t} + \varepsilon\mathbf{u}\cdot\nabla\left(\rho_{\mathrm{f}}(T_{\mathrm{f}}, p)c_{p,\mathrm{f}}(T_{\mathrm{f}}, p)T_{\mathrm{f}}\right) = \nabla\cdot\left(\varepsilon k_{\mathrm{f}}(T_{\mathrm{f}}, p)\nabla T_{\mathrm{f}}\right) + q_{\mathrm{sf}}\left(T_{\mathrm{s}} - T_{\mathrm{f}}\right) \tag{3}$$

$$(1-\varepsilon)\frac{\partial\left(\rho_{\mathrm{s}}c_{p,\mathrm{s}}(T_{\mathrm{s}}, \mu_0 H)T_{\mathrm{s}}\right)}{\partial t} = \nabla\cdot\left((1-\varepsilon)k_{\mathrm{s,eff}}(T_{\mathrm{s}})\nabla T_{\mathrm{s}}\right) + q_{\mathrm{sf}}\left(T_{\mathrm{f}} - T_{\mathrm{s}}\right) + \dot{Q}_{\mathrm{MCE}} \tag{4}$$

The energy equation of helium in the expansion chamber is as follows.

$$\frac{\partial\left(\rho_{\mathrm{f}}(T_{\mathrm{f}}, p)c_{p,\mathrm{f}}(T_{\mathrm{f}}, p)T_{\mathrm{f}}\right)}{\partial t} + \mathbf{u}\cdot\nabla\left(\rho_{\mathrm{f}}(T_{\mathrm{f}}, p)c_{p,\mathrm{f}}(T_{\mathrm{f}}, p)T_{\mathrm{f}}\right) = \nabla\cdot\left(k_{\mathrm{f}}(T_{\mathrm{f}}, p)\nabla T_{\mathrm{f}}\right) \tag{5}$$

where, $\boldsymbol{u}$=(u, v) is the velocity vector of helium. T_f and T_s are the temperature of helium and regenerator material respectively. p is the pressure of helium. $\rho_f(T_f, p)$, $c_{p,f}(T_f, p)$, $k_f(T_f, p)$ and $\mu_f(T_f, p)$ are the density, the specific heat capacity, the thermal conductivity and the dynamic viscosity of helium respectively. They are functions of temperature and pressure and derived by REFPROP database. ε is the porosity of regenerator. q_{sf} is the interstitial convection heat transfer coefficient between the helium and regenerator materials. ρ_s, $c_{p,s}(T_s, \mu_0 H)$ and $k_{s,eff}(T_s)$ are the density, the specific heat capacity and the effective thermal conductivity of regenerator material, respectively. The physical properties of Pb and ErNi are taken from references [12, 15]. $\dot{Q}_{MCE}$ is a heat source to describe the magnetocaloric effect of ErNi.

It is worth mentioning here that in the practical packed bed regenerator, the solid particles are in point contact with each other, and the contact thermal resistance between particles cannot be ignored. Especially for such kind of small-scale liquid helium temperature refrigerator with less than 1 W of cooling power, it is inaccurate to directly use the thermal conductivity of a bulk solid as the default setting in the COMSOL porous media model, which will lead to a large deviation in the estimation of cooling power because solid heat conduction from the high temperature end to the low temperature end calculated in this way is an order of magnitude higher than the cooling power. In this model, a modified thermal conductivity, i.e., $k_{s,eff}(T_s)$ is used by multiplying the thermal conductivity with a degradation factor, which is usually about 0.1.

2.3 Boundary conditions

The boundary conditions at the high temperature end of the regenerator (top of the regenerator) are given as follows.

$$T_{\mathrm{f,\,top}} = T_0,\; p_{\mathrm{top}} = p_0(t),\; y_{\mathrm{top}} = 0 \tag{6}$$

where, T_0 is the inlet temperature of the helium, which has given in Table 1. $p_0(t)$ is the pressure curve, as shown by the solid line in Fig. 2 [16]. y_{top} is the displacement at the high temperature end.

The boundary conditions at the end of the expansion chamber are as follows.

$$\left(\frac{\partial T_{\mathrm{f}}}{\partial y}\right)_{\mathrm{bottom}} = 0,\; \left(\frac{\partial p}{\partial y}\right)_{\mathrm{bottom}} = 0,\; y_{\mathrm{bottom}} = y_0(t) \tag{7}$$

$y_0(t)$ is the displacement curve at the bottom of the expansion chamber, as shown by the dotted line in Fig. 2. Moving meshes is used to simulate the displacement. When $y_0(t)$ is 0, the bottom of the expansion chamber is at the lowest point, and the volume of the expansion space is the largest.

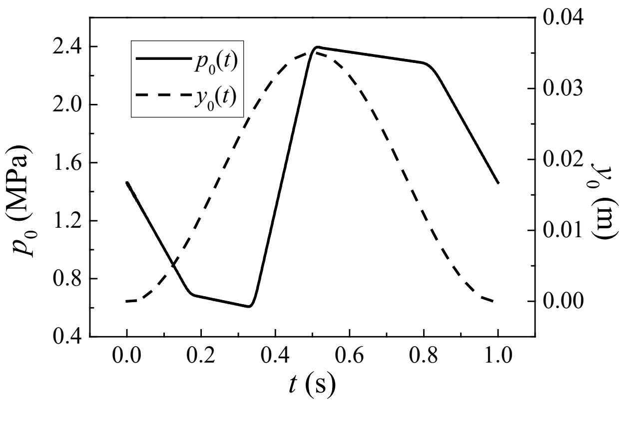

Fig. 2 Boundary conditions of pressure at the top of the regenerator and stroke at the bottom of the expansion chamber

3. Simulation results and discussion

With the hybrid refrigeration model, the effect of the timing between gas expansion and magnetic refrigeration is studied and optimized. The corresponding cooling capacity and efficiency are obtained and compared with the results from pure gas expansion. For a complete evaluation, the eddy current loss of the cold head was estimated numerically to be about 0.1 W at a frequency of 1 Hz and was included in the following simulations. The efficiency mentioned later is the second thermodynamic efficiency, which is the ratio of the coefficient of performance (COP) of the system to the ideal COP. In this model, the ideal COP is defined as the Carnot efficiency between the high and low temperature end of the second stage regenerator, i.e., 45 K and 4~8 K.

To describe the timing between the two refrigeration effects, a phase angle is defined as the phase difference between the maximum value of varying magnetic field and the minimum value of varying expansion chamber volume. Fig. 3 shows the displacement curve (solid line) at the bottom of the expansion chamber and the magnetic field curve (dotted line), the corresponding phase angle is 60° as a typical example here [14]. With the eddy current loss considered, the no-load temperature at different phase angles are simulated. Fig. 4 shows numerical and experimental results of the no-load temperature at different phase angles. The curve variation trend of the numerical simulation is in agreement with experimental results. The numerical results show that the optimal phase angle is 90°, and the corresponding no-load temperature reaches 2.45 K.

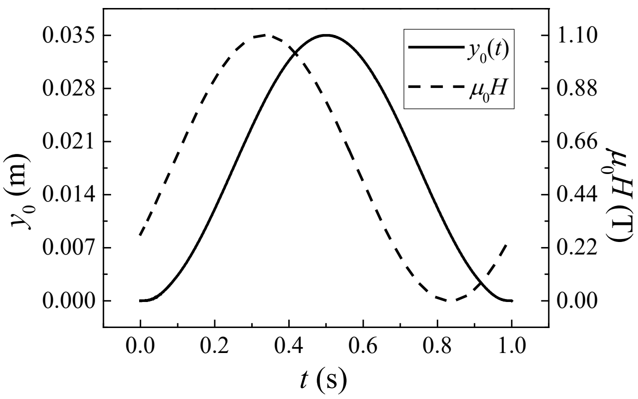

Fig. 3 Displacement curve (solid line) at the bottom of the expansion chamber and magnetic field curve (dotted line)

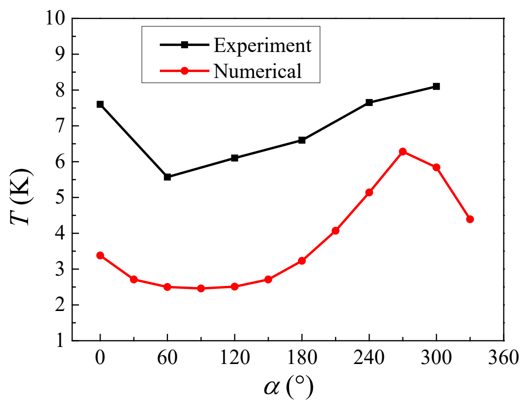

Fig. 4 Numerical and experimental results of the no-load temperature at different phase angles

The performance of the hybrid refrigeration at optimal phase angle is simulated and compared with the

GM refrigeration. Fig. 5 and Fig. 6 respectively shows the cooling power and the efficiency of the hybrid refrigerator as well as the GM refrigeration as a function of temperature at 1 Hz. As the temperature increases, the cooling power and the efficiency increase. Regardless of the eddy current loss, the cooling power of the hybrid refrigeration at 4 K is 0.37 W and the efficiency is 9.27%, which are 2.85 and 2.92 times that of GM refrigeration, respectively. With the eddy current loss considered, the cooling power and the efficiency of the hybrid refrigeration at 4 K are 2.07 and 2.13 times higher than that of GM.

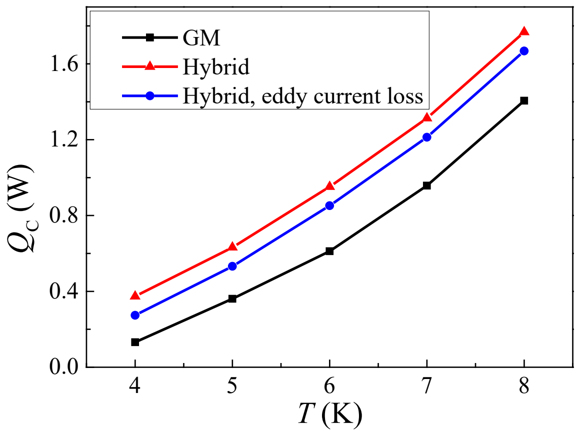

Fig. 5 Numerical results of the cooling power at different temperatures

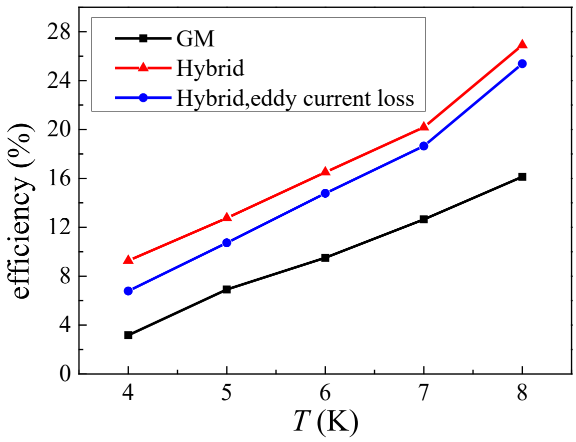

Fig. 6 Numerical results of the efficiency at different temperatures

4. Conclusion

In this paper, a hybrid refrigeration model combining gas expansion and magnetic refrigeration is proposed using COMSOL Multiphysics. The effect of the timing between gas expansion and magnetic refrigeration is studied and optimized. The corresponding cooling capacity and efficiency are obtained and compared with the results from pure gas expansion. The numerical results show that the optimal phase angle is 90°. At the optimal phase angle, the cooling power and efficiency at 4 K are respectively 2.07 times and 2.13 times of GM. If the eddy current loss of cold head can be effectively suppressed, the performance can be further improved. This numerical simulation provides guidance for optimizing the performance of hybrid refrigerator.

5. References

[1] Mcmahon H O, Gifford W E. A New Low-Temperature Gas Expansion Cycle[J]. Advance in cryogenic engineering, 1960, 5:354-367.
[2] Nagao M, Inaguchi T, Yoshimuro H, et al. Helium liquefaction by a Gifford-McMahon cycle cryocooler[J]. Advances in cryogenic engineering, 1990, 35:1251-1260.
[3] Ackermann R A, Herd K G, Chen W E. Advanced Cryocooler Cooling for MRI Systems[J]. Cryocoolers, 1999, 10:857-867.
[4] Radenbaugh R. Refrigeration for superconductors[J]. Proceedings of the IEEE, 2004, 92(10):1719-1734.
[5] Radebaugh R. Cryocoolers: the state of the art and recent developments[J]. Journal of Physics: Condensed Matter, 2009, 21(16):164219.
[6] V.K. Pecharsky, K.A. Gschneidner Jr, Magnetocaloric effect and magnetic refrigeration, Journal of Magnetism and Magnetic Materials, 200 (1999) 44-56.
[7] Giauque W F, MacDougall D P. Attainment of temperatures below 1° absolute by demagnetization of $Gd_2(SO_4)_3 \cdot 8H_2O$[J]. Physical Review 1933, 43:768.
[8] Yu B F, Gao Q, Zhang B, et al. Review on research of room temperature magnetic refrigeration[J]. International Journal of Refrigeration, 2003, 26(6):622-636.
[9] Jeong S, Smith Jr J L. Magnetically Augmented Regeneration in Stirling Cryocooler[J]. Advances in Cryogenic Engineering, 1994, 39:1399-1405.
[10] Nellis G F, Smith Jr J L. Design of an Experimental Apparatus for Investigation of a Stirling/Magnetic Cycle[J]. Advances in Cryogenic Engineering, 1996, 41:1665-1673.
[11] Nellis G F, Smith Jr J L. An Experimental GM/Magnetic Refrigerator[J]. Advances in Cryogenic Engineering, 1998, 43:1767-1774.
[12] Yayama H, Hatta Y, Tomokiyo A, et al. Specific Heat of ErNi in Magnetic Fields and Its Performance as Regenerator Material in Gifford-McMahon Refrigerator at Cryogenic Temperatures[J]. Japanese Journal of Applied Physics, 1996, 35(10):5545-5549.
[13] Yayama H, Hatta Y, Makimoto Y, et al. Hybrid cryogenic refrigerator: combination of Brayton magnetic-cooling and Gifford-McMahon gas-cooling system[J]. Japanese Journal of Applied Physics, 2000, 39(7):4220-4224.
[14] Jun Shen, Xinqiang Gao, Ke Li, Wei Dai, Zhenxing Li, Zhaojun Mo, Xinqi Zheng, Maoqiong Gong. Experimental research on a 4 K hybrid refrigerator combining GM gas refrigeration effect with magnetic refrigeration effect[J]. Cryogenics, 2019, 99:99-104.
[15] Ogawa M, Li R, Hashimoto T. Thermal conductivities of magnetic intermetallic compounds for cryogenic regenerator[J]. Cryogenics, 1991, 31(6):405-410.
[16] Inaguchi T, Nagao M, Naka K, et al. Numerical Simulation of 4K GM Refrigerator[J]. Cryocoolers, 2002, 2000(4):593-602.